UDC 539.4

Analysis of Warm Prestressing Effect on Fracture Toughness of Reactor Pressure Vessel Steels

R. Beleznai and Sz. Szávai

Bay Zoltan Foundation for Applied Research, Institute for Logistics and Production Systems, Miskolc-Tapolca, Hungary

УДК 539.4

Оценка влияния предварительной горячей опрессовки сосудов давления реакторов на вязкость разрушения реакторных сталей

Р. Белезнаи, Ш. Шаваи

Фонд прикладных исследований им. Золтана Бая, Институт логистики и промышленных систем, Мишкольц-Тапольца, Венгрия

Выполнен конечноэлементный расчет напряженно-деформированного состояния образцов типа Шарпи с трещиной при испытаниях на трехточечный изгиб с учетом влияния предварительной горячей опрессовки на вязкость разрушения реакторных сталей. При этом использовались два различных закона упрочнения материала. Для каждого случая получены расчетные значения J-интеграла и проведен их сравнительный анализ.

Ключевые слова: сосуды давления реактора, предварительная горячая опрессовка, конечный элемент, закон упрочнения, *J*-интеграл.

Introduction. The presented research work is connected to a running project NESC-VII, which is a European cooperative action in support of warm prestressing (WPS) usage in the reactor pressure vessel (RPV) integrity assessment. WPS is a phenomenon which justifies that crack does not propagate during unloading cycle in case of PTS. Bay Zoltan Foundation for Applied Research (BZF) takes part in the modeling work where the WPS effects on *J*-integral should be determined. In the first stage of the project, a preliminary calculation has been performed. The discussed problem is very actual, since many nuclear power plants are getting closer to the end of their lifetime. The keypoint of lifetime extension projects is to determine which method should be applied, in order to ensure the expected safety service period. The purpose of this project is to assess the WPS effect on RPV steel properties. Scarce data are available on WPS, and it is known that this phenomenon improves fracture toughness of materials. However, the mechanism of this effect is not explained yet, although much research has been dedicated to this issue. Within framework of this project, two different material hardening laws are compared, in order to estimate the one which describes better the mechanical behavior under WPS conditions.

Material Properties. Study of specimens under WPS condition has been performed on 18MND5 (A533B) ferritic steel. The material has been manufactured according to the RCC-M specifications by Creusot Loire Industrie in 1995. The chemical composition is given in Table 1. The material properties are provided by AREVA NP [1].

Table 1

Chemical Composition of 18MND5 Steel

C	Mn	Si	Ni	Cr	Mo	Cu	S	P	Al	V
0.19	1.5	0.23	0.66	0.17	0.485	0.084	<0.001	0.004	0.011	0.004

True strain–stress curves from −150 to 20°C are available for the calculation. These curves have been extrapolated to large strains using the Hollomon type relation, e.g.:

$$\sigma = K(\varepsilon^p)^n, \tag{1}$$

where σ is the stress, ε^p is the plastic strain, and K and n are material coefficients. These parameters and Young's modulus values of 18MND5 ferritic steel for different temperatures are given in Table 2.

Table 2

Variation of the Hollomon Relation Parameters and Young's Modulus in the Temperature Range from −196 to 20°C

Temperature (°C)	K (MPa)	n	E (GPa)
−196	1592.3	0.154	213.6
−150	1424.3	0.173	211.1
−120	1389.6	0.196	209.7
−100	1317.9	0.198	208.9
−50	1181.9	0.167	207.1
−20	1057.9	0.139	206.2
20	1056.7	0.155	205.3

The type of hardening for this steel (isotropic or kinematic) is not clear. Anyway, if we assume this hardening to be a purely kinematic one, the following hardening law can be used:

$$\begin{cases} (\sigma - X)_{eq} = \sigma_0, \\ X = \dfrac{2}{3} C\alpha, \quad \dot{\alpha} = \dot{\varepsilon}^p - \gamma\alpha\dot{p}. \end{cases} \tag{2}$$

Two parameters C and γ, as well as the yield strength σ_0 of this hardening law have been fitted (see Table 3) to the experimental tensile curves (−150 to 20°C range):

$$\sigma = \sigma_0 + \frac{C}{\gamma}[1 - \exp(-\gamma \varepsilon^p)], \tag{3}$$

where σ and ε^p are the axial stress and plastic strain, respectively.

Table 3

Evolution of the Material Parameters (Kinematic Hardening Law) with Temperature

Temperature (°C)	−150	−100	−50	−20	20
σ_0, MPa	765.0	623.0	570.0	547.0	517.0
C, MPa	2430.0	2710.0	3470.0	3360.0	3640.0
γ	4.4	4.9	7.7	8.7	12.0

Finite Element Model of Three-Point Bending Specimen. Precracked Charpy-like three-point bending (3PB) specimen geometry without side-grooving was chosed for the analysis. The dimensions are the following: $630 \times 85 \times 40$ mm. The specimen contained a crack with ratio $a/W = 0.34$ (a is crack length and W is specimen width). In the present analysis, both hardening laws were examined, in order to determine which is more appropriate to describe material behavior during the unloading.

2D finite element model was generated in MSC.MARC2007R1 code using 8-nodal quadratic elements. The mesh of the half part of the specimen is presented in Fig. 1. Plain strain condition was used in the analysis. The mesh was refined around the crack front. *J*-integral was calculated based on the virtual crack extension (VCE) method implemented into the software and with the help of analytical formulas based on load–load line displacement (LLD) curve developed by the VOCALIST project [2].

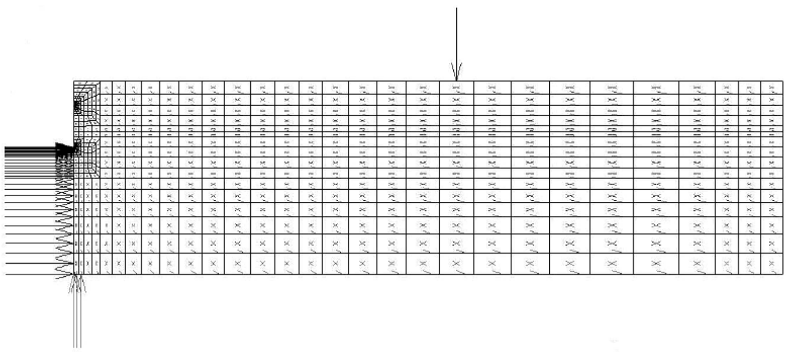

Fig. 1. Mesh of the large-scale Charpy-like 3PB specimen.

The following formula was applied for determination of the *J*-integral values:

$$J = J_e + J_{pl}, \tag{4}$$

where

$$J_e = \frac{K^2 (1 - \nu^2)}{E}. \tag{5}$$

The elastic part (K) is calculated according to ASTM 1921 [6], the plastic part (J_{pl}) – according to formula:

$$J_{pl} = \eta_{pl} \frac{A_{pl}}{B_n(W - a_0)} \tag{6}$$

with

$$A_{pl} = \int_0^{LLD_{pl}} Pd(LLD_{pl}). \tag{7}$$

For SE(B) specimens with standard cracks ($a/W \sim 0.5$), $\eta_{pl} = 1.9$.
For shallow crack ($a/W \sim 0.1$),

$$\eta_c = 0.32 + 12\left(\frac{a_0}{W}\right) - 49.5\left(\frac{a_0}{W}\right)^2 + 99.8\left(\frac{a_0}{W}\right)^3. \tag{8}$$

The ratio $a/W = 0.34$, which is closer to deep crack, was chosen for further calculation. The WPS conditions were the following: in the first cycle (loading and unloading, LU), the temperature was constant $T = 20$°C, after unloading the temperature was decreased to $T = -150$°C without mechanical load, and then a LU cycle followed at constant temperature $T = -150$°C. The temperature and load distribution diagrams can be seen in Figs. 2 and 3. The post-processed LLD curve is given in Fig. 4. From this it can be concluded that plastic region of the loading is very large.

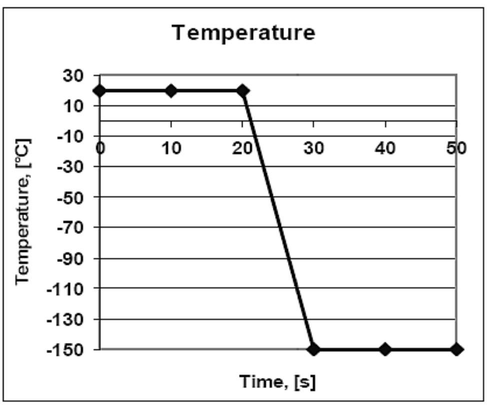

Fig. 2

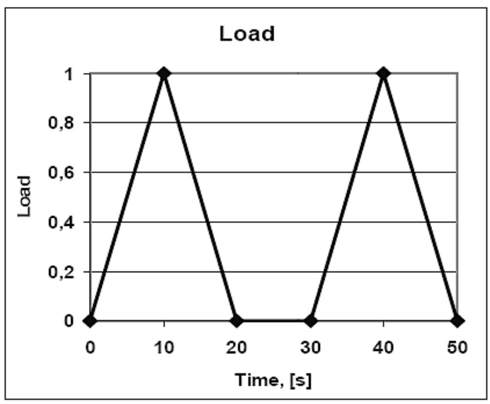

Fig. 3

Fig. 2. Temperature distribution during the loading process.
Fig. 3. Load cycles during the analysis.

Results. J-integral was plotted in time for the WPS loading cycles. The finite element calculation results and the analytical solution were compared for both hardening laws (Fig. 5). In case of isotropic hardening law, the J-integral value is much higher than in the other case, and after unloading a residual part of J-integral

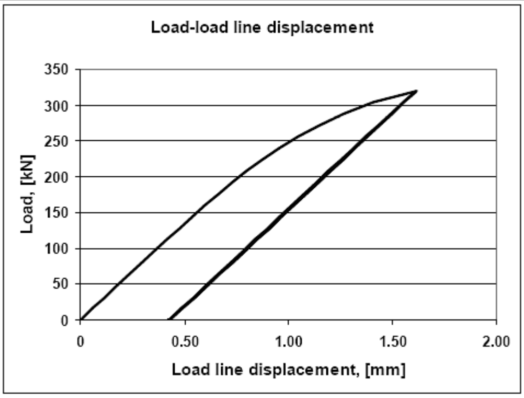

Fig. 4. Load–load line displacement curves.

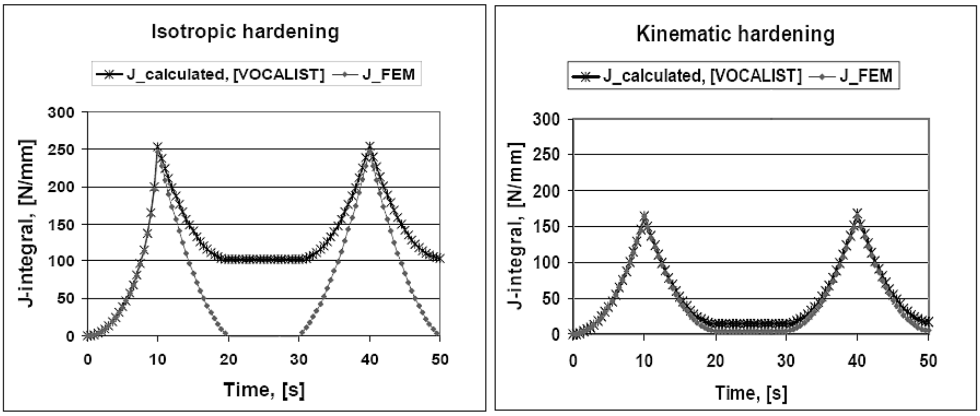

a *b*

Fig. 5. *J*-integral curves under WPS condition in case of different hardening laws.

is present. This causes the difference between the two results. The reason of this is that isotropic hardening law is not appropriate in unloading stage. To draw the conclusion from this, kinematic hardening law should be applied for further analysis. The WPS effect can arise from the fact that preliminary high-level loading (close to the ultimate stress) caused changes in the crystalline structure of the material, and the initially homogenous isotropic texture will become anisotropic with higher fracture toughness. Right now this is only an assumption and further investigation is necessary.

Conclusions. The finite element calculation of precracked Charpy-like 3PB specimen has been performed to analyze the effect of WPS on *J*-integral value of reactor pressure vessel steel. Two different hardening laws were applied in the calculation, and it can be concluded that kinematic hardening law is more appropriate for WPS analysis, because in the unloading cycle the isotropic hardening parameters fail to appropriately describe the material behavior. From the calculated *J*-integral one can be see a slight tendency that *J*-integral value is increased due to the WPS effect. However, the mechanism of the WPS is an open issue yet. Therefore, further investigations are required with 3D finite element models for different specimen geometries.

Р е з ю м е

Виконано скінченноелементний розрахунок напружено-деформованого стану зразків типу Шарпі з тріщиною при випробуваннях на триточковий згин з урахуванням впливу попереднього гарячого опресування на в’язкість руйнування реакторних сталей. При цьому використовували два різних закони зміцнення матеріалу. Для кожного випадку отримано розрахункові значення *J*-інтеграла та проведено їх порівняльний аналіз.

1. *NESC VII Project: Presentation of Data Necessary for the Feasibility Test Predefinition*, AREVA NP, France (2008).
2. *Validation of Constraint Based Assessment Methodology in Structural Integrity*, VOCALIST Project Report (2004).

Received 21. 06. 2009